# Protein kinase-D1 overexpression prevents lipid-induced cardiac insulin resistance

Journal of Molecular and Cellular Cardiology 76 (2014) 208–217

Contents lists available at ScienceDirect

Journal of Molecular and Cellular Cardiology

journal homepage: www.elsevier.com/locate/yjmcc

Original article

# Protein kinase-D1 overexpression prevents lipid-induced cardiac insulin resistance

Ellen Dirkx [a], Guillaume J.J.M. van Eys [a], Robert W. Schwenk [a], Laura K.M. Steinbusch [a], Nicole Hoebers [a], Will A. Coumans [a], Tim Peters [b], Ben J. Janssen [c], Boudewijn Brans [d], Andreas T. Vogg [e], Dietbert Neumann [a], Jan F.C. Glatz [a], Joost J.F.P. Luiken [a,*]

[a] Department of Molecular Genetics, Cardiovascular Research Institute Maastricht (CARIM), Maastricht University, The Netherlands
[b] Department of Experimental Cardiology, Cardiovascular Research Institute Maastricht (CARIM), Maastricht University, The Netherlands
[c] Department of Pharmacology, Cardiovascular Research Institute Maastricht (CARIM), Maastricht University, The Netherlands
[d] Department of Nuclear Medicine, Maastricht University Medical Center, The Netherlands
[e] Department of Nuclear Medicine, University Hospital Aachen, Germany

ARTICLE INFO

*Article history:*
Received 18 July 2014
Received in revised form 19 August 2014
Accepted 21 August 2014
Available online 28 August 2014

*Keywords:*
Cardiomyopathy
Fatty acid transport
Glucose transport
Insulin resistance
Protein kinase D

ABSTRACT

In the insulin resistant heart, energy fuel selection shifts away from glucose utilization towards almost complete dependence on long-chain fatty acids (LCFA). This shift results in excessive cardiac lipid accumulation and eventually heart failure. Lipid-induced cardiomyopathy may be averted by strategies that increase glucose uptake without elevating LCFA uptake. Protein kinase-D1 (PKD1) is involved in contraction-induced glucose, but not LCFA, uptake allowing to hypothesize that this kinase is an attractive target to treat lipid-induced cardiomyopathy. For this, cardiospecific constitutively active PKD1 overexpression (caPKD1)-mice were subjected to an insulin resistance-inducing high fat-diet for 20-weeks. Substrate utilization was assessed by microPET and cardiac function by echocardiography. Cardiomyocytes were isolated for measurement of substrate uptake, lipid accumulation and insulin sensitivity. Wild-type mice on a high fat-diet displayed increased basal myocellular LCFA uptake, increased lipid deposition, greatly impaired insulin signaling, and loss of insulin-stimulated glucose and LCFA uptake, which was associated with concentric hypertrophic remodeling. The caPKD1 mice on high-fat diet showed none of these characteristics, whereas on low-fat diet a shift towards cardiac glucose utilization in combination with hypertrophy and ventricular dilation was observed. In conclusion, these data suggest that PKD pathway activation may be an attractive therapeutic strategy to mitigate lipid accumulation, insulin resistance and maladaptive remodeling in the lipid-overloaded heart, but this requires further investigation.


## 1. Introduction

Heart disease, often presenting as cardiomyopathy, is the leading cause of death among patients with type-2 diabetes [1,2]. It is the metabolic component of diabetes that has been increasingly implicated as the primary factor leading to cardiac dysfunction in these patients [3,4]. In particular, altered substrate utilization by the heart has been recently positioned as causative to the development of diabetic cardiomyopathy [3,5].

GLUT4 and CD36 are the main cardiac glucose and long-chain fatty acid (LCFA) transporters, respectively, and are critical regulatory sites in substrate utilization [5–7]. In the healthy heart, both GLUT4 and CD36 are stored in endosomal compartments, from where these transporters can translocate to the sarcolemma to increase glucose and LCFA uptake. GLUT4 and CD36 translocation appear to be similarly regulated, since the same physiological stimuli, i.e., circulating insulin levels and increased contractile activity, induce their simultaneous translocation to the sarcolemma [8].

The diabetic heart displays increased LCFA utilization at the expense of glucose. The greater influx of LCFA is due to a permanent CD36 relocation from intracellular stores to the sarcolemma [5], and results in the gradual myocellular build-up of triacylglycerols (TAG), diacylglycerols (DAG) and other lipid species. Especially, DAG activate Ser/

*Abbreviations:* AMPK, AMP-activated protein kinase; AW, anterior wall; BNP, B-type natriuretic peptide; caPKD1, cardiospecific constitutively active PKD1 overexpression; DAG, diacylglycerol; EFS, electric field stimulation; [$^{18}$F]FDG, [$^{18}$F]fluoro-deoxyglucose; [$^{18}$F]FTHA, 14(R,S)-[$^{18}$F]fluoro-6-thia-heptadecanoic acid; GSK3, glycogen synthase kinase-3; HDAC5, histone deacetylase-5; LCFA, long-chain fatty acids; LFD, low fat diet; LV, left ventricular; microPET, micro-positron emission tomography; PKD1, protein kinase-D1; SUV, standardized uptake value; TAG, triacylglycerol; WD, Western diet; WT, wild-type.

* Corresponding author at: Maastricht University, Department of Molecular Genetics, Cardiovascular Research Institute Maastricht (CARIM), P.O. Box 616, 6200 MD Maastricht, The Netherlands. Tel.: +31 43 3881209, +31 43 3884574; fax: +31 43 3884574.
*E-mail address:* j.luiken@maastrichtuniversity.nl (J.J.F.P. Luiken).

http://dx.doi.org/10.1016/j.yjmcc.2014.08.017
0022-2828/

Thr-kinase cascades, which impair upstream insulin signaling, and subsequently reduce insulin-stimulated glucose uptake [9]. Over time, both excessive lipid accumulation and progressive insulin resistance will gradually initiate a remodeling process in the heart, which at first appears to be a compensatory adaptation, but which thereafter turns maladaptive [10,11].

Strategies to stimulate glucose uptake in the diabetic heart, without increasing LCFA uptake, may be well suited to restore the substrate balance and combat the diabetic state. Insulin-induced GLUT4 translocation is defective in the type-2 diabetic heart [12]. Therefore, activation of signaling mechanisms involved in contraction-induced GLUT4 translocation may be excellent targets to increase cardiac glucose utilization during insulin resistance [13]. We expect that greater glucose influx into the diabetic heart would counterbalance excessive lipid usage, and eventually recuperate contractile function [5].

One of the best-studied proteins in the signaling events induced by contraction is AMP-activated protein kinase (AMPK). Unfortunately, AMPK stimulates not only the translocation of GLUT4 to the sarcolemma but simultaneously also that of CD36 [14]. Thus, AMPK activation would not be capable of shifting the excessive LCFA utilization in the insulin resistant heart towards a more balanced utilization of glucose and LCFA.

Another kinase involved in contraction-induced GLUT4 translocation is protein kinase-D1 (PKD1). This kinase is the defining member of a novel class of Ser/Thr kinases belonging to the PKD family [15]. Recently, we have shown that PKD1 is activated by contraction [16]. Importantly, silencing of PKD1 in HL1-cardiomyocytes resulted in loss of contraction-induced glucose uptake whereas contraction-induced LCFA uptake was retained [17]. Hence, we hypothesized that activation of this kinase would shift cardiac substrate utilization towards glucose.

Cardiospecific overexpression of PKD1 in mice on a normal diet leads to hypertrophy, ventricular dilatation and impaired systolic function [18]. This maladaptive hypertrophic remodeling is associated with and thought to be due to increased phosphorylation of HDAC5, a direct substrate of PKD [19]. Subsequently, this phosphorylation disattaches HDAC5 from the hypertrophic transcription factor MEF2, thereby inducing the transcription of MEF2-regulated hypertrophic genes [20]. Notwithstanding these adverse effects of PKD1 upregulation in hearts of mice under a normal diet regime, PKD1 overexpression might still be beneficial in the lipid-overloaded insulin resistant heart to counterbalance the impairment in glucose uptake. Therefore, we subjected mice cardiospecifically overexpressing PKD1 to a Western diet (WD) in order to investigate whether increased expression/activity of this kinase would be protective against lipid-induced insulin resistance and lipid-induced cardiac remodeling.

## 2. Materials and methods

### 2.1. Animals

Cardiac-specific constitutively active PKD1 overexpression (caPKD1) mice were a kind gift from Prof. Dr. Eric Olson (University of Texas Southwestern Medical Center, Dallas, USA). Breeding was performed with founder pairs of heterozygous mice. Both male and female mice were taken from a restricted number of nests, containing wild type as well as transgenic animals. From earlier studies with cardiomyocytes or hearts from wild-type (WT) mice and various transgenic mouse models, we found that metabolic and signaling parameters were not different between both sexes [14,16,17,21]. From the age of 12 weeks, caPKD1 mice were administered with a low fat diet (LFD) containing 10 en% fat (D12450B, Research Diets) or WD containing 45 en% fat (D12451, Research Diets). For this, male and female mice were divided over the different experimental groups as unpaired littermates. In all experiments in this study, the number of male and female mice was about equal. Animals were maintained at the Experimental Animal Facility of Maastricht University, and had free access to food and water. All study protocols involving the animal experiments were approved by the Animal Care and Use Committee of Maastricht University and were performed according to the official rules formulated in the Dutch law on care and use of experimental animals, highly similar to those of the US National Institutes of Health (NIH Publication No. 85-23, revised 1996).

### 2.2. Blood glucose and insulin levels

After 4 h of fasting, blood was collected via the tail vein. To measure blood glucose levels, a blood glucose monitor was used (OneTouch Ultra, Milpitas, CA, USA). Insulin plasma levels were measured by performing an insulin ELISA (Millipore, Billerica, MA, USA).

### 2.3. Isolation and treatment of adult mouse cardiomyocytes

Cardiomyocytes were isolated from male and female WT (C57BL/6) or transgenic mice as previously described [21]. Briefly, mice were anesthetized via one intraperitoneal injection with pentobarbital (120 mg/kg body mass; pharmacy of the Faculty of Veterinary Medicine, Utrecht, Netherlands). Then, these mice were examined on the adequacy of the anesthesia via monitoring eye and leg reflexes. Hearts were excised and perfused using a Langendorff perfusion system and Liberase blendzyme-1 (Roche Diagnostics, Indianapolis, IN) for isolation of cardiomyocytes. Upon 90 min of recovery after the isolation procedure, cardiomyocytes were subjected to electric field stimulation (EFS)[1] for 4 min at 37 °C (2 Hz, 40 V, pulse duration 10 msec) or incubated with 100 nM insulin for 15 min. Cellular uptake of [$^3$H]deoxyglucose and [$^{14}$C]palmitate was measured as previously described [21]. In short, 0.5 ml of a mixture of [1-$^{14}$C]palmitate/BSA complex and [1-$^3$H] deoxyglucose was added at the start of the incubations so that the final concentration of both substrates amounted to 100 μM with a corresponding palmitate/BSA ratio of 0.3. Cellular uptake was determined after 5 min, which time point is within the initial uptake phase (i.e., the phase in which uptake of both substrates proceeds linearly with time). Within this phase there is no release of $CO_2$, which production starts at >10 min after [1-$^{14}$C]palmitate addition [22]. For assessment of substrate uptake, cells were washed three times in an ice-cold stop solution containing 0.2 mM phloretin, and subsequently lysed in 5 ml Opti-Fluor scintillation fluid (PerkinElmer, Waltham, USA).

### 2.4. Immunoblotting

Proteins were separated by SDS-PAGE (4–12% Bis-Tris Criterion XT precast gels; Biorad, Hercules, USA) and transferred to nitrocellulose membranes for Western blotting. The protein bands were visualized as previously described [16]. Antibodies against Akt (phospho-Ser473), caveolin-3, ERK1/2 (phospho-Thr202/Tyr204), glycogen synthase kinase-3β (phospho-Ser9), mammalian target of rapamycin (phopho-Ser2448), p38 (phospho-Thr180/Tyr182), p70 S6 kinase (phospho-Thr389), PKD1 and PKD1 (phospho-Ser744/748) were purchased from Cell Signalling Technologies (Danvers, USA). The antibody directed against GLUT4 was obtained from Santa Cruz Biotechnology (Santa Cruz, USA), the antibody against mouse CD36 was from Chemicon (Billerica, USA), and the antibodies against phospho-Ser498-histone deacetylase-5 and the OXPHOS complexes were from Abcam (Cambridge, UK).

### 2.5. RT-PCR

Total RNA was isolated from snap frozen heart tissue using the mirVana Isolation Kit (Ambion) and treated with DNase I (DNA-free, Ambion) to remove residual DNA. 700 ng of the total RNA was reverse transcribed using the miScript II RT Kit (Qiagen). RT-qPCR was performed using SybrGreen (Bio-Rad) and the following primer sequences (5′ → 3′): GTTTGGGCTGTAACGCACTGA (Bnp-F), GAAAGAGACCCAGG CAGAGTCA (Bnp-R), CGCTTCGGCAGCACATATAC (U6-F) and TTCACG AATTTGCGTGTCAT (U6-R).

### 2.6. Intramyocardial triacylglycerol

Intramyocellular lipids were extracted from snap frozen cardiomyocytes and separated by high-performance thin layer chromatography [23]. Bands were resolved with a hexane/diethylether/propanol (87:10:3) solution stained with MnCl2/H2SO4 in methanol. Triacylglycerol bands were detected with a Molecular Imager (ChemiDoc XRS, Bio-rad, California, USA) and analyzed with Quantity One® (Biorad, California, USA).

### 2.7. Hematoxylin–eosin staining

Morphology of the heart was visualized using hematoxylin–eosin staining of paraffin sections from both WT and caPKD1 mice on LFD or WD.

### 2.8. Echocardiography

Transthoracic echocardiographic measurements were performed under 1–2% isoflurane anesthesia using a RMV707B (15–45 M Hz) scan-head interfaced with a Vevo-770 high frequency ultrasound system (VisualSonics Inc., Toronto, Canada). Long-axis EKG-triggered cine loops of the left ventricular (LV) contraction cycle were obtained in B-mode to assess end-diastolic/systolic volume. Short-axis recordings of the LV contraction cycle were taken in M-mode to assess wall thickness of the anterior/posterior wall at the mid-papillary level. From B-mode recordings, LV length from basis to apex, LV internal diameter in systole (LVIDs) and diastole (LVIDd) were determined, and the ejection fraction was calculated from the latter two parameters. From M-mode recordings, LV anterior wall thickness in systole (AWths) and diastole (AWthd) were determined.

### 2.9. Micro-positron emission tomography

[$^{18}$F]Fluoro-deoxyglucose ([$^{18}$F]FDG) was obtained from GE Healthcare Radiofarmaca, Eindhoven. 14(R,S)-[$^{18}$F]fluoro-6-thia-heptadecanoic acid ([$^{18}$F]FTHA) has been manually prepared using the precursor 14-(R,S)-tosyloxy-6-thiaheptadecanoic acid benzyl ester purchased from ABX (Radeberg, Germany). Four GBq [$^{18}$F]fluoride have been concentrated and purified using a Sep-Pak® Light QMA cartridge (Waters, Milford, MA, USA) preconditioned with $NaHCO_3$. The fixed activity was eluted with 600 μL of a solution containing 207 μL 0.04 M $K_2CO_3$ and 393 μL 95 mM Kryptofix 2.2.2 (Merck, Germany) in $CH_3CN$. The effluent was evaporated to dryness in a 2 mL V vial within 25 min at 95 °C in a nitrogen gas stream. This procedure was repeated three times following a re-dissolution with 500 mL $CH_3CN$, respectively. The final residue was cooled and 200 μL of a solution of 45 mM precursor in $CH_3CN$ was added. Labeling was achieved within 15 min at 95 °C. Subsequent saponification was conducted within 10 min at 95 °C after addition of 150 μL 1 M NaOH to the crude mixture. When finished, a mixture of 75 mL HOAc and 75 mL $CH_3CN$ was added. Purification was performed using a polymeric RP phase HPLC column (PRP-1, 5 μm, 250 × 3mm, CS-Chromatographie, Langerwehe, Germany) and eluent 86% $CH_3CN$ aq with 0.5% HOAc at a flow rate of 1 mL/min (260 bar). [$^{18}$F]FTHA (3–4 min) eluted after [$^{18}$F]Fluride (1.5–3 min). Product fraction was evaporated at 82 °C, dissolved in 50 μL EtOH and diluted with 150 μL PBS and further with 500 μL saline. The overall radiochemical yield was 31% and synthesis time was 3 h. All mentioned chemicals were of analytical grade. Quality control was performed using TLC plates (aluminium backed silica gel 60, Merck, Darmstadt, Germany) and eluent hexane:ethyl acetate:acetic acid = 75:25:0.1. [$^{18}$F]FTHA had a $R_f$ value of 0.45. Radiochemical purity was 92.4 ± 3.5% (n = 6).

The radiopharmaceuticals were all given after a 3 hour fasting. For determination of in vivo glucose uptake into the heart, the mice received an intraperitoneal injection of a mean of 0.34 MBq/g body weight [$^{18}$F]FDG (range 0.32–0.37) in a first set of experiments (Fig. 1). The excellent image characteristics in these experiments allowed a lower dose of 0.16 MBq [$^{18}$F]FDG (mean value; range 0.12–0.23) to be given in a second set of experiments (Fig. 3A). For determination of in vivo cardiac LCFA uptake, the mice received an intravenous injection of 0.13 MBq/g [18F]FTHA (range 0.08–0.20). One hour after injection of either of both substrates, a 30 min image acquisition was performed. Mice were scanned with a microPET system (Focus 120, Siemens, Erlangen, Germany) with an axial field of view of 7.6 cm consisting of 95 slices of 0.796 mm thick. The spatial resolution was 1.4 mm at the center of the field of view. During acquisition, mice were maintained under 2% isoflurane anesthesia. After the experiment, mice were weighted. Cardiac [$^{18}$F]FDG and [$^{18}$F]FTHA uptake was quantified in a volume of interest consisting of the whole heart, and expressed as standardized uptake value (SUV) obtained by calculating the ratio of myocardial activity to injected dose, normalized by body weight.

### 2.10. Data presentation and statistics

All results are presented as means ± SEM. Data presented in Fig. 1A were analyzed using the unpaired Student's t-test. In all other figures, data were analyzed by two-way ANOVA, and significant differences between groups were determined with Bonferroni post-hoc tests. When evaluating the signaling/metabolic effects of insulin within each animal group, we used the paired t-test (Figs. 4B–D). Two-sided values of $P < 0.05$ were considered significant.

## 3. Results

### 3.1. Metabolic characterization of hearts/cardiomyocytes from mice with cardiospecific constitutively active PKD1 overexpression

CaPKD1 mice were injected with [$^{18}$F]FDG. MicroPET imaging of these mice showed a higher level of cardiac glucose accumulation than WT mice (Fig. 1A). Subsequently, cardiomyocytes were isolated from these mice and used for analysis of PKD1 signaling and of substrate transporters. Cardiospecific PKD1 overexpression leads to elevated basal levels of PKD1 phosphorylation/activation, and additionally to phosphorylation of its well-identified target protein [20] histone deacetylase-5 (HDAC5) (Fig. 1B). In contrast, protein levels of GLUT4 and CD36 were similar to WT (Fig. 1B), indicating that cardiospecific PKD1 overexpression does not affect substrate transporter expression. Cardiospecific PKD1 overexpression also did not affect various signaling pathways, such as AMPK signaling, mitogen-activated protein kinase signaling (phosphorylation of ERK1/2 and p38), calcium/calmodulin-dependent protein kinase (CaMK)-II signaling, protein kinase C (PKC)-δ and PKC-θ phosphorylation, as well as phosphorylation of mammalian target of rapamycin (and its substrate p70 S6 kinase) (Fig. 1B). Additionally, cardiomyocytes were subjected to EFS, and subsequently used for assessment of substrate uptake. In caPKD1 cardiomyocytes, basal glucose uptake was increased by 1.5-fold compared to WT cardiomyocytes, and EFS-stimulated glucose uptake by 1.4-fold (Fig. 1C). Basal and EFS-stimulated LCFA uptake in caPKD1 cardiomyocytes were not different from WT (Fig. 1C). We conclude that PKD1 is involved in the regulation of cardiac glucose uptake, but does not act on LCFA uptake.

### 3.2. Effects of PKD1 overexpression and high-fat diet on signaling and substrate uptake in cardiomyocytes

WT- and caPKD1 mice were subjected to a WD regime over a period of 20 weeks to induce (whole-body) insulin resistance and cardiomyopathy. This diet regime induced increased body mass (Fig. 2A), blood glucose (Fig. 2B), and plasma insulin levels (Fig. 2C) in both WT- and caPKD1 mice. Cardiospecific PKD1 overexpression did not improve total body insulin sensitivity, given

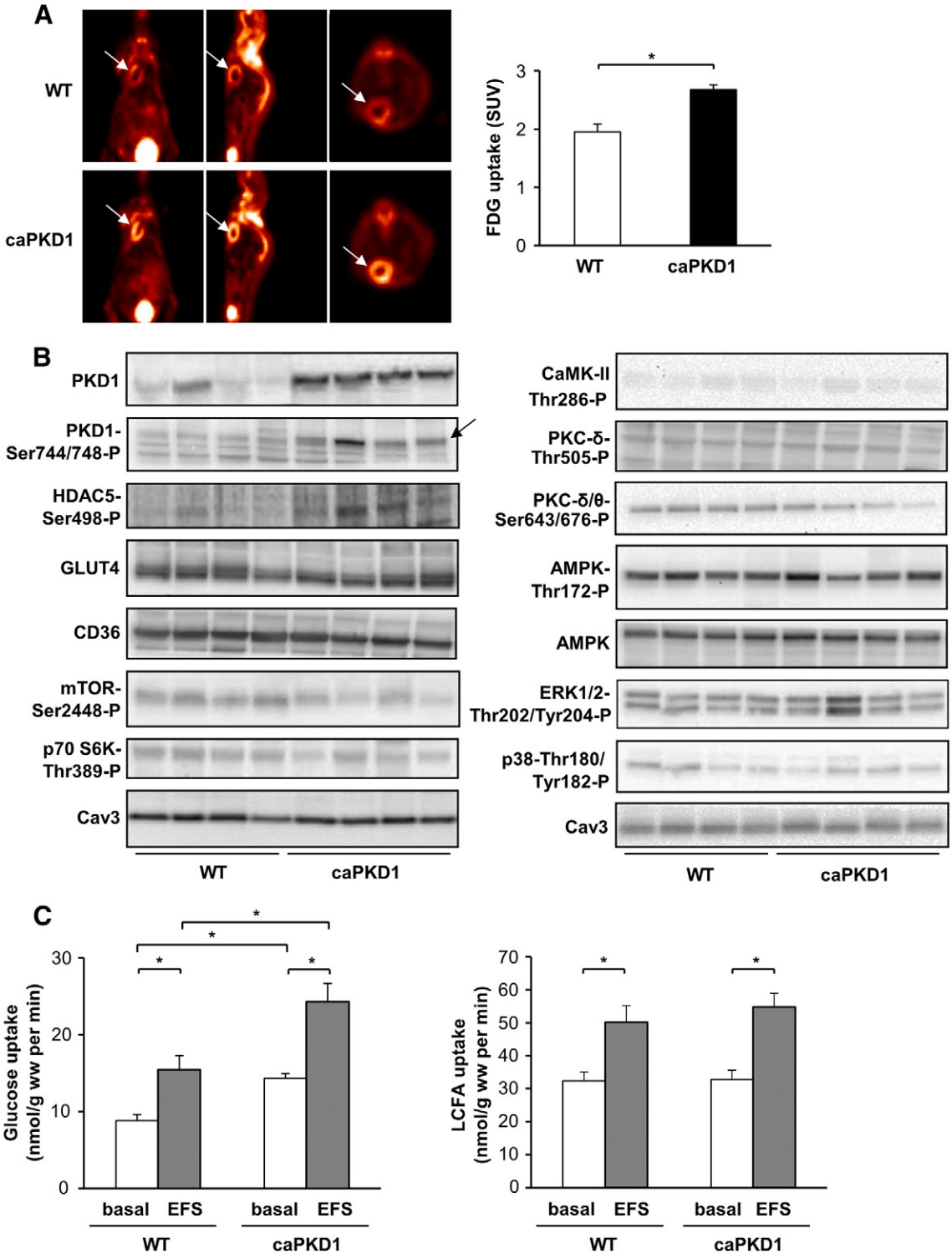


**Fig. 1.** PKD1 is essential for glucose uptake but not for LCFA uptake. (A) At the age of 12 weeks WT (n = 5) and caPKD1 mice (n = 5) were injected with [$^{18}$F]FDG followed after 1 h by 30 min microPET scanning. Cardiac uptake of [$^{18}$F]FDG in both WT and caPKD1 mice was visualized (left panels). Representative images show coronal, sagittal and transverse view of a WT and caPKD1 mouse. All corresponding PET scans are displayed with the same magnification factor. The arrows indicate the heart. Images were quantified by standardized uptake values (SUV) (right panel). (B) Primary cardiomyocytes were isolated from 12 week old WT (n = 6) and caPKD1 mice (n = 6). A portion of these cells were used for Western analysis of PKD1, GLUT4, CD36 and AMPK expression, compared to caveolin-3 (loading control), and also of phosphorylation of HDAC5, mammalian target of rapamycin (mTOR), p70 S6 kinase (S6K), PKC-δ, PKC-θ, AMPK, CaMK-II, ERK1/2 and p38 MAPK. (C) The remainder of these cells were incubated in the absence and presence of electric field stimulation (EFS), and subsequently used for measurement of [$^{14}$C]palmitate and [$^{3}$H]glucose uptake (n = 6 for both animal groups). *Statistically different ($p < 0.05$).

that there were no significant differences in blood glucose and plasma insulin levels between the WT-WD and caPKD-WD groups (Figs. 2B,C).

In vivo measurement of myocardial substrate uptake in WT mice revealed the tendency of myocardial glucose uptake to decrease by the WD condition (−31%, $P > 0.05$), while myocardial LCFA uptake

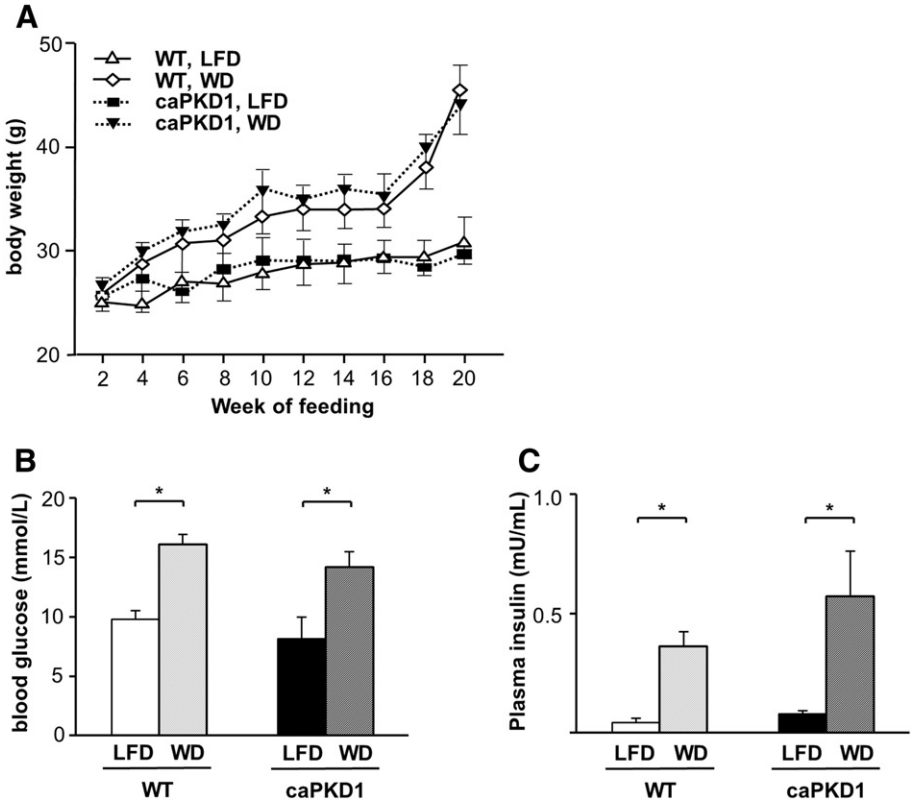


**Fig. 2.** High-fat diet administration to WT and caPKD1 mice induces obesity and whole-body insulin resistance. After 20 weeks of WD feeding, (A) body mass (WT-LFD, n = 13; WT-WD, n = 14; caPKD1-LFD, n = 12; caPKD1-WD, n = 11), as well as (B) fasted blood glucose levels (WT-LFD, n = 9; WT-WD, n = 9; caPKD1-LFD, n = 4; caPKD1-WD, n = 6) and (C) fasted plasma insulin levels (n = 4 for all animal groups) were determined. *Statistically different ($p < 0.05$).

concomitantly increased by 1.7-fold (Fig. 3). Relative to their WT littermates, in the LFD condition the caPKD1 mice showed enhanced myocardial glucose uptake by 2.2-fold and decreased myocardial LCFA uptake by 58% (Fig. 3). However when subjected to WD, myocardial glucose and LCFA uptake of caPKD1 mice were similar to WT-LFD group (Fig. 3).

In cardiomyocytes from WT mice, administration of WD induced characteristics of lipid-induced insulin-resistance such as intramyocellular TAG and DAG accumulations (2.5-fold and 1.5-fold, respectively; Fig. 4A), complete loss of insulin-stimulated phosphorylation of Akt and of the Akt-substrate glycogen synthase kinase-3 (GSK3)α/β (Fig. 4B), decreased insulin-stimulated glucose uptake (−55%; Fig. 4C) and a 2.3-fold elevated basal cardiac LCFA uptake rate (Fig. 4D). This elevation in basal LCFA uptake was accompanied by a loss of insulin-stimulated LCFA uptake ((Fig. 4D), but not by an alteration in CD36 expression (Fig. 4E). Basal glucose uptake into cardiomyocytes (Fig. 4C) and expression of GLUT4 and the OXPHOS complexes (Fig. 4E) were not altered by WD. In cardiomyocytes from the caPKD1-LFD group, the signaling, metabolic and mitochondrial parameters were not much different from WT-LFD cardiomyocytes (Fig. 4), except for a 1.9-fold increase in TAG content and a 1.4-fold increase in basal glucose uptake (Figs. 4A,C). In particular, DAG content, insulin signaling and the insulin-stimulated component in myocellular glucose and LCFA uptake remained unaltered in caPKD1-LFD if compared to WT-LFD (Figs. 4A–D). However, remarkably, caPKD1-WD cardiomyocytes displayed signaling and metabolic parameters strikingly dissimilar to WT-WD but closely resembling those found in WT-LFD cardiomyocytes (Fig. 4). Therefore, the signaling and metabolic abnormalities observed in caPKD1-LFD hearts diminished in the WD condition. Corresponding data from WT-LFD and caPKD1-WD mice were similar.

### *3.3. Effects of PKD1 overexpression and high-fat diet on cardiac morphology and function*

Morphological examination demonstrated concentric hypertrophic remodeling of WT-WD hearts (Fig. 5A). Echocardiographic measurements of WT-WD mice disclosed signs of LV concentric hypertrophic remodeling, such as increased LV wall thickness and decreased LV internal and external diameters (Figs. 5B,C). These LV morphological changes were accompanied by increased ejection fraction and fractional shortening (Fig. 5C; fractional shortening is deduced from LV internal and external diameters: data not shown). In contrast, hearts from caPKD1 mice on LFD showed eccentric cardiac hypertrophy (Figs. 5A,B) and decreased cardiac function (Fig. 5C). These alterations in cardiac structure and function, seen in caPKD1 mice on LFD, were consistent with previously reported dilated cardiomyopathy [18]. On the other hand, cardiac morphology and function in caPKD1 mice on WD were similar to those of WT mice on LFD (Fig. 5). No concentric or dilated hypertrophy was observed (Figs. 5A,B), and ejection fraction was not decreased (Fig. 5C). These findings confirm the previously observed cardiac hypertrophy of caPKD1 mice on LFD, whereas cardiac function and morphology of the same mice on WD regime presents in the normal range, i.e. similar to WT-LFD.

### *3.4. Effects of PKD1 overexpression and high-fat diet on HDAC5 phosphorylation*

Based on the postulated involvement of HDAC5 in the development of cardiac hypertrophy in the caPKD1-LFD mice (see Introduction), we determined PKD1-HDAC5 signaling in all experimental groups. First, please note that changes in PKD1-Ser744/748 phosphorylation

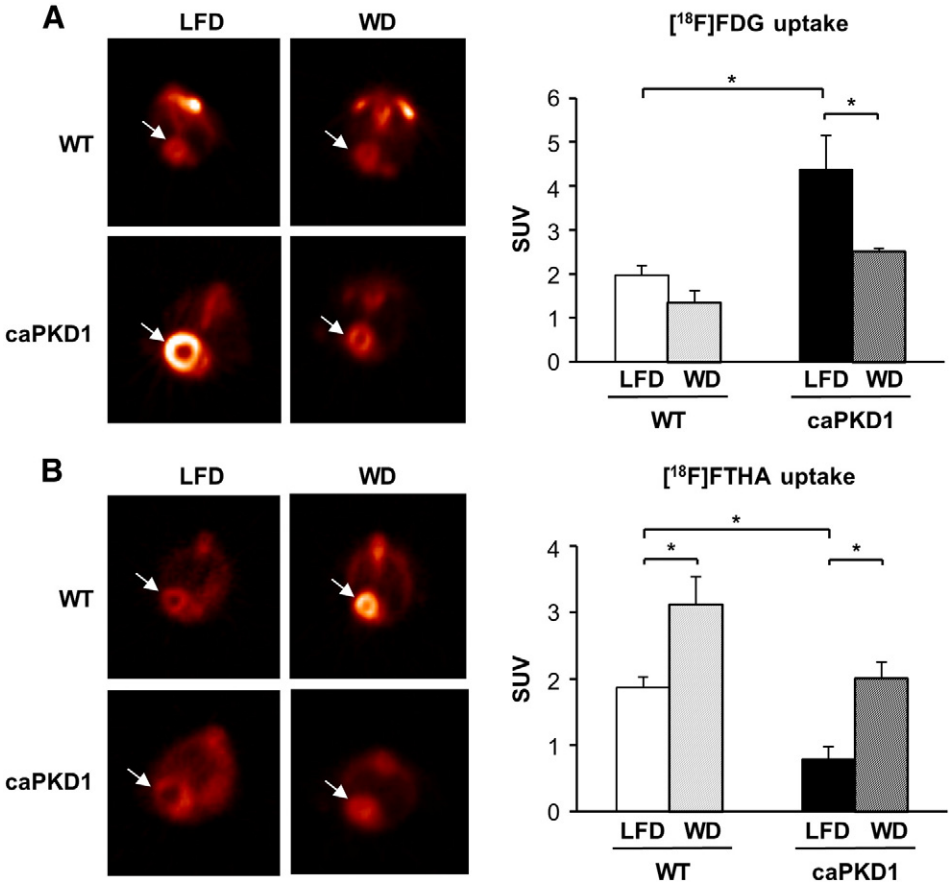


**Fig. 3.** Substrate uptake in caPKD1 mice on a high fat diet is normalized. Using microPET imaging, in vivo glucose and LCFA uptake were measured in WT and caPKD1 mice on LFD and WD. These mice were injected with [$^{18}$F]FDG (WT-LFD, n = 6; WT-WD, n = 5; caPKD1-LFD, n = 6; caPKD1-WD, n = 5) and [$^{18}$F]FTHA (n = 6 for all animal groups), followed after 1 h by 30 min microPET scanning. All PET scans are displayed with the same magnification factor. Representative images visually show cardiac uptake of (A) [$^{18}$F]FDG and (B) [$^{18}$F]FTHA in both WT and caPKD1 mice (left panel, arrows indicate the heart), as well as quantitatively by standardized uptake values (SUV) (right panel). *Statistically different ($p < 0.05$).

occurred proportionally to changes in total PKD expression (Fig. 6). In WT hearts, the WD regime decreased the phosphorylation of PKD1 and of its substrate HDAC5 by 56% and 73%, respectively. Cardiospecific overexpression of PKD1 enhanced PKD1 and HDAC5 phosphorylation by 3.6-fold and 1.7-fold, respectively (Fig. 6, in agreement with Fig. 1). Additionally, cardiospecific PKD1 overexpression elevated the transcription of B-type natriuretic peptide (BNP), an established marker for cardiac hypertrophy [18]. In caPKD1 hearts, WD reduced PKD1 phosphorylation by 32%, HDAC5 phosphorylation by 72%, and BNP transcription by 86% (Fig. 6). Importantly, the levels of HDAC5 phosphorylation and BNP transcription in caPKD-WD hearts were not higher than in WT-LFD hearts. Hence, the WD-induced dephosphorylation of HDAC5 might provide a mechanism for the abolishment of the eccentric hypertrophy in caPKD1-WD hearts.

## 4. Discussion

We investigated the effects of WD on the PKD1 overexpressing mouse heart. The three main findings are: (i) In caPKD1 mice cardiac substrate uptake shifts from LCFA towards increased glucose usage. (ii) The WD regime rescues the abnormalities in morphology and function of PKD1 overexpressing hearts, whereas conversely (iii) PKD1 overexpression prevents cardiac lipid overload and insulin resistance, as observed upon WD feeding in WT mice.

The cardiomyopathy in caPKD1 mice is apparent at the age of one month [18]. Therefore, the WD regime that started three months after birth acts to restore the heart rather than to prevent disease occurrence. Indeed after 20 weeks of WD, caPKD1 mice displayed a normal heart morphology, function and metabolism thus pointing to complete regression. In an attempt to clarify the molecular mechanism that underlies this WD-mediated recovery, we determined HDAC5 signaling, which previously has been suggested as responsible for pathological remodeling in the caPKD1 heart [18]. Interestingly, WD inhibits myocardial HDAC5 phosphorylation in both WT and caPKD1 mice (Fig. 6). In caPKD1-WD hearts, this return to the non-phosphorylated state would re-allow HDAC5 to bind to the hypertrophy-associated transcription factor MEF2, and thereby suppress MEF2 from driving the hypertrophic gene program [20]. Accordingly, elevated transcription of the hypertrophic gene BNP in caPKD1-LFD hearts was reversed on WD. In conclusion, these findings support a role for HDAC5 and MEF2 in the eccentric remodeling in caPKD1 hearts. However, in the concentric hypertrophy (i.e., increased LV wall thickness and increased mass together with decreased LV chamber volume) that occurs in WT-WD hearts, HDAC5 phosphorylation is reduced, suggesting that the PKD1–HDAC5–MEF2 pathway is not involved in this type of hypertrophy.

Metabolic imaging using microPET showed that caPKD1 mice exhibit increased cardiac glucose import and decreased LCFA uptake. We did not observe significantly altered expression levels of OXPHOS complexes, GLUT4 or CD36 (Figs. 1 and 4E), indicating that mitochondrial oxidative capacity or total tissue transporter contents do not contribute to the observed substrate shift. Previously, we observed that PKD1 silencing in HL-1 cardiomyocytes resulted in the loss of EFS-stimulated GLUT4 translocation as well as of EFS-stimulated glucose uptake, whereas CD36 translocation and LCFA uptake were retained [17]. These findings were confirmed in cardiomyocytes from cardiospecific PKD1 knockout mice [17]. In the present study, using caPKD1

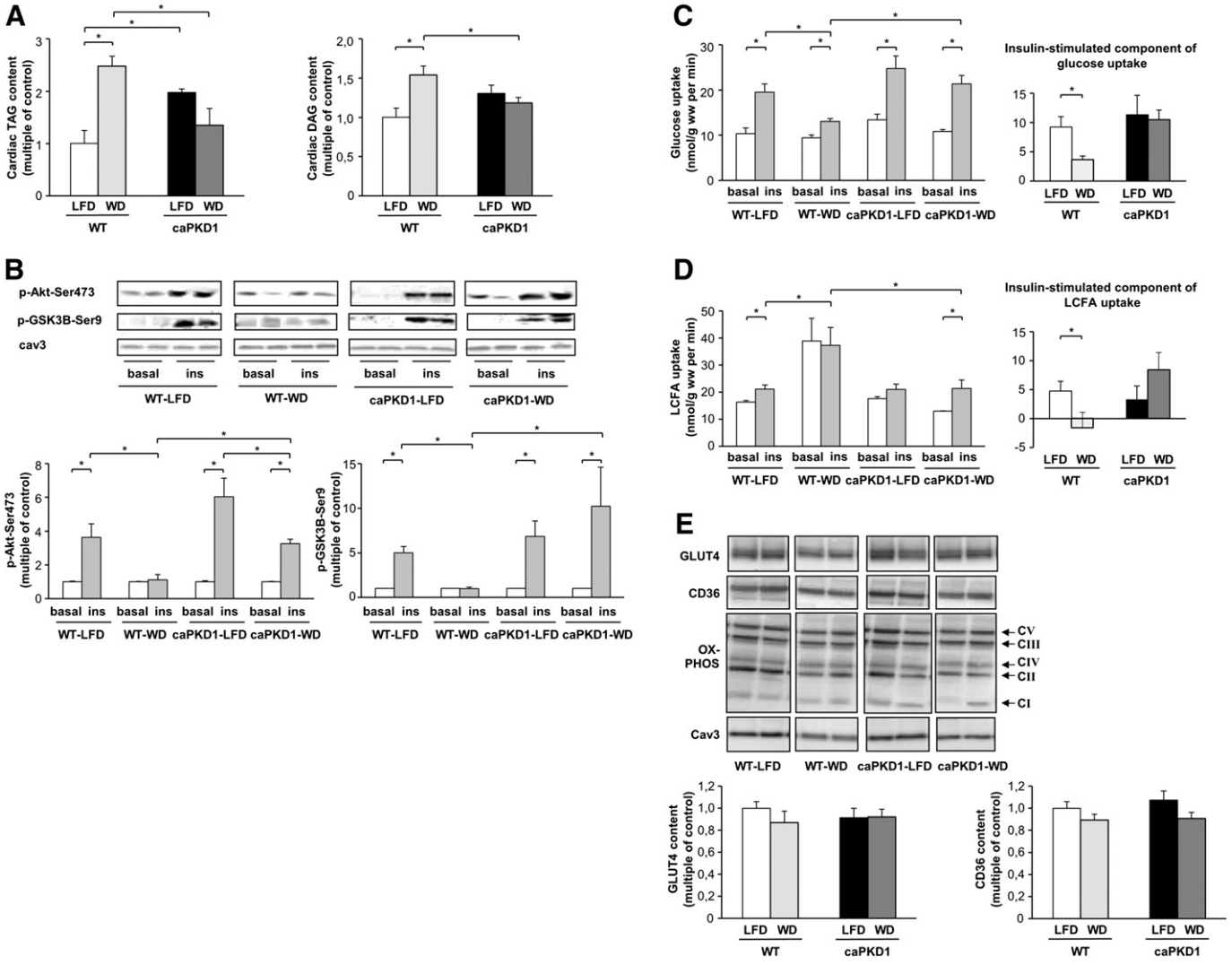


**Fig. 4.** Hearts from caPKD1 mice are protected against high-fat diet-induced lipid accumulation and insulin resistance. At the end of a period of 20 weeks of diet, WT and caPKD1 mice on LFD and WD were sacrificed for isolation of primary cardiomyocytes. (A) Determination of intracellular TAG and DAG content (WT-LFD, n = 6; WT-WD, n = 7; caPKD1-LFD, n = 4; caPKD1-WD, n = 5). The TAG and DAG levels were normalized against the WT-LFD groups. Absolute TAG and DAG levels were 12.5 ± 2.9 and 5.5 ± 0.8 mg/g wet mass, respectively. (B, C) Primary cardiomyocytes were challenged with insulin (ins; 100 nM; 15 min), and subsequently used for (B) Western blot detection of Akt-Ser473-phosphorylation (n = 6 for all animal groups) and GSK3α/β-Ser9 phosphorylation (n = 4 for all animal groups), and (C) for uptake of [$^3$H]deoxyglucose and (D) [$^{14}$C]palmitate (WT-LFD, n = 7; WT-WD, n = 7; caPKD1-LFD, n = 7; caPKD1-WD, n = 5). In case of Akt and GSK3α/β phosphorylation, the insulin-induced changes have been normalized against the basal level within each group. For both glucose and LCFA uptake, the insulin-stimulated component was calculated (ins-basal) and displayed in the corresponding right panels. (E) Hearts were also used for preparation of tissue lysates and subsequent Western detection of CD36, GLUT4 and OXPHOS proteins (complexes I–V; CI–CV) (n = 4 for all animal groups). *Statistically different ($p < 0.05$).

cardiomyocytes, we obtained reciprocal evidence for the specific involvement of PKD1 in glucose uptake, because basal and EFS-stimulated glucose uptakes were elevated whereas basal and EFS-stimulated LCFA uptake remained unaltered. Therefore, the increase in basal glucose uptake is associated with upregulation of basal PKD1 phosphorylation/activity and enhanced basal glucose import, which most likely corresponds to enhanced basal GLUT4 translocation. Collectively, these findings firmly establish a role of PKD1 in contraction-stimulated cardiac glucose uptake in vivo.

Besides the PKD1–HDAC5–MEF2 pathway, the development of eccentric cardiac hypertrophy could also be due to the shift in cardiac substrate preference towards glucose [24]. Therefore, the elevated glucose uptake in caPKD1-LFD vs. WT-LFD hearts may help to explain the observed cardiomyopathy. However, the PKD1-mediated increase in glucose uptake may not be substantial enough to trigger cardiac hypertrophy. Namely, GLUT1 transgenic mice (displaying an increase in myocardial glucose utilization of a similar magnitude) did not develop cardiac hypertrophy and dysfunction [25]. Hence, the PKD1–HDAC5–MEF2 pathway seems sufficient to explain the development of eccentric cardiac hypertrophy in our animal model. Nevertheless, our data clearly indicate that the increased glucose uptake rates of caPKD1-LFD hearts return to normal levels in the WD condition. Vice versa, the diminished LCFA uptake in caPKD1-LFD hearts restores with WD. Therefore, the cardiac substrate balance is associated with cardiac health in line with previous findings [26,27].

In wild-type animals the WD regime enhanced body mass and circulating glucose and insulin levels, indicating obesity and peripheral insulin resistance. However, cardiospecific PKD1 overexpression did not influence these maladaptive changes at the whole body level. Furthermore, in WT hearts, the WD condition induced well known features of lipid-induced cardiomyopathy. Cardiomyocytes from these WD-fed mice displayed elevated basal LCFA uptake together with a loss of insulin-stimulated LCFA uptake while total CD36 expression was unaltered. We also observed this pattern of alterations in other rodent models of cardiac lipid-induced insulin resistance [5,28,29], and deduced the following sequence of events. One of the first alterations in the heart exposed to lipids is the permanent relocation of CD36 from insulin-responsive endosomal stores to the sarcolemma. The

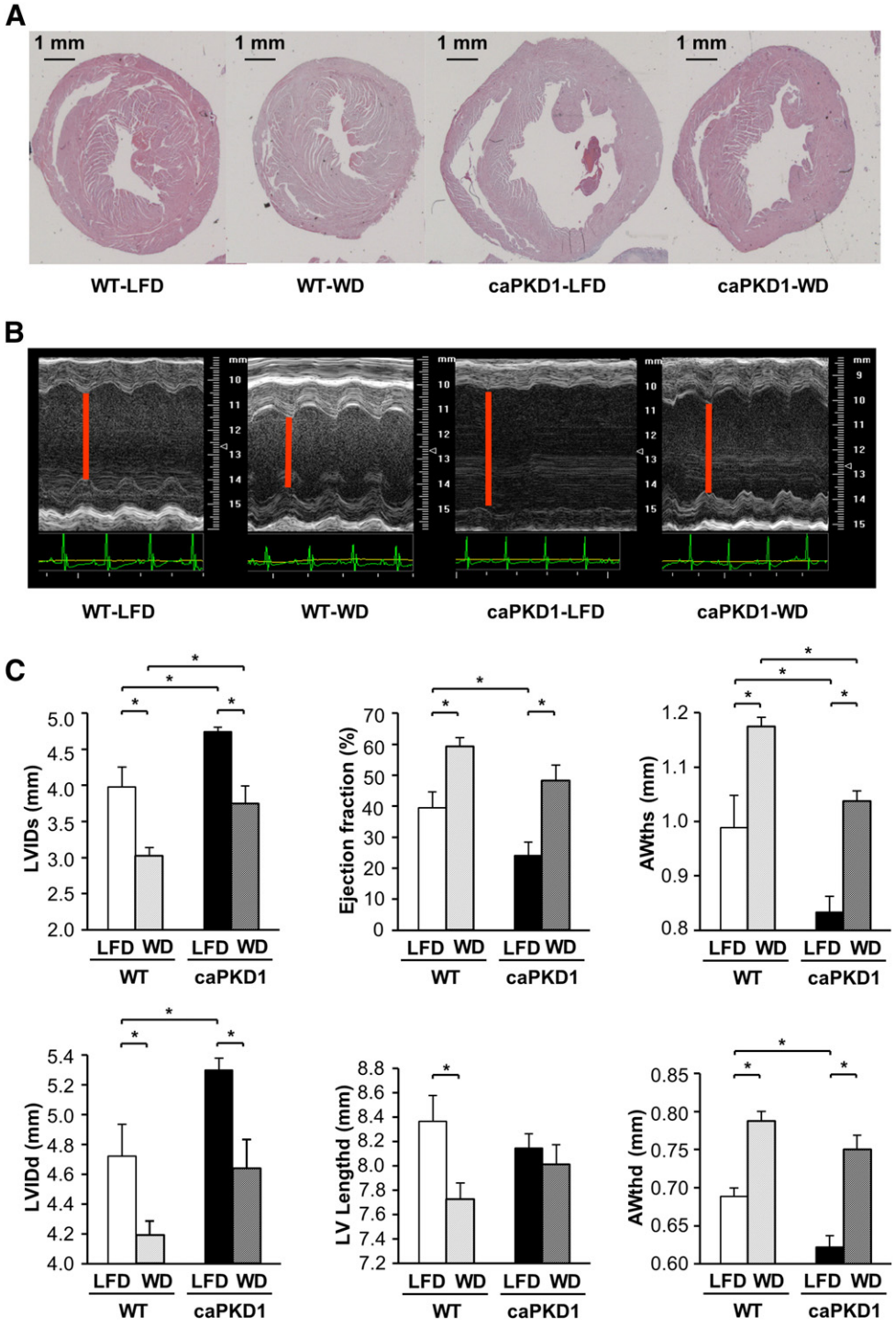


**Fig. 5.** Effects of cardiac PKD1 overexpression and high-fat diet on cardiac morphological and functional parameters. WT and caPKD1 mice on LFD and WD were analyzed after 20 weeks of diet. (A) The morphology of the hearts was visualized with a hematoxylin–eosin staining of the heart. (B, C) Echocardiography measurements. (B) Representative M-mode images are displayed. (C) From M-mode recordings, LV anterior wall thickening in systole (AWths) and diastole (AWthd) were determined. From B-mode recordings LV internal diameter in systole (LVIDs) and diastole (LVIDd) were determined, and ejection fraction was calculated from these parameters. In these same recordings, LV length from basis to apex was determined. Values represent averages of following animal groups: WT-LFD, n = 9; WT-WD, n = 8; caPKD1-LFD, n = 9; caPKD1-WD, n = 8. *Statistically different ($p < 0.05$).

consequent chronical increase in LCFA uptake will exceed the mitochondrial β-oxidative capacity, and, by default, result in myocellular accumulation of bio-active lipid intermediates (DAG), which in turn will impair insulin signaling, insulin-stimulated GLUT4 translocation and glucose uptake [9]. Ultimately, there will be a shift from glucose to LCFA utilization in cardiomyocytes from WT mice exposed to the WD regime, as was confirmed with microPET imaging in vivo. After 20 weeks of WD, hearts of WT mice displayed concentric hypertrophy. Remarkably, also the ejection fraction increased. This form of hypertrophy to increase cardiac output might be one of the earliest morphological alterations in diabetic cardiomyopathy, and would initially be compensatory to the increase in total body mass upon Western lifestyle (lipid overconsumption). Accordingly, subjects with impaired glucose tolerance (early sign of development of type-2 diabetes) exhibited increased left ventricular mass and wall thickness as well as higher cardiac output compared to glucose tolerant subjects [10]. Likely, these humans

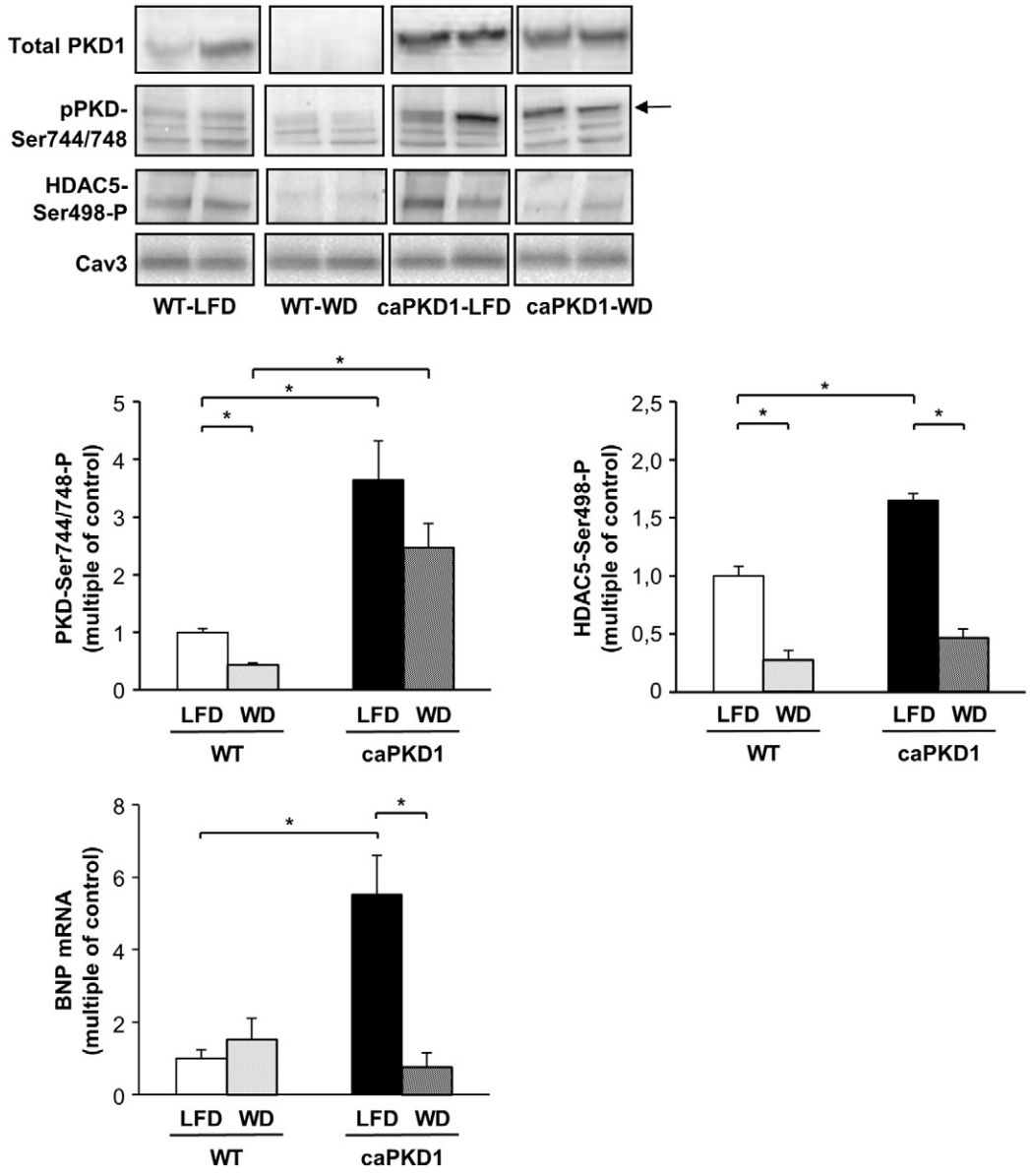


**Fig. 6.** The WD regime suppresses cardiac HDAC5 phosphorylation. At the end of a period of 20 weeks of diet, WT and caPKD1-mice on LFD or WD were sacrificed for preparation of heart tissue lysates and subsequent Western detection of total and phosphorylated PKD1 and HDAC5, compared to caveolin-3 (loading control) ($n = 4$ for all animal groups). Additionally, snap frozen heart tissue was used for RT-PCR detection of BNP. BNP expression was normalized for U6 mRNA levels; see Materials and methods *Statistically different ($p < 0.05$).

in the early stages of cardiac remodeling would be expected to develop overt diabetic cardiomyopathy upon continuation of their lifestyle [11]. Similarly, we documented previously that continuation of the WD regime in rodents would lead to a sequence of maladaptive alterations in both cardiac morphology and function [29]. The underlying mechanisms responsible for this WD/obesity-related concentric hypertrophic remodeling are not known [30].

In contrast to WT mice on WD, caPKD1 mice on WD exhibited normal basal LCFA uptake and intramyocellular DAG and TAG levels. Additionally, in caPKD1-WD hearts, insulin signaling and insulin-induced glucose uptake remained at the levels of WT-LFD. Hence, PKD1 activation could be suggested as a possible treatment strategy aiming at increased glucose import into the insulin resistant heart. Furthermore, it remains to be shown whether PKD activation in a high fat environment to prevent hypertrophy is a therapeutic target. However, this present study employed ectopic overexpression of constitutively active PKD1 in rodent heart, which under normal diet conditions resulted in dilated cardiomyopathy (as discussed above). Clearly, an acute model of PKD1 overexpression or activation is required to test PKD1 as a drug target for possible cardio-metabolic treatment. Moreover, PKD1 has been previously implicated in multiple important cellular processes ranging from insulin secretion to cell proliferation [31,32]. In summary, PKD1 appears to be less attractive as a drug target. However, the pathway downstream of PKD1 would show a higher potential for treatment strategies and thus remain in our focus. Therefore, future research should be aimed at identifying the proteins downstream of PKD1 and specifically involved in GLUT4 translocation.

## Disclosures

None.

## Acknowledgments

We are thankful to the Professors Eric N. Olson and Rhonda Bassel-Duby (University of Texas Southwestern Medical Center, Dallas, USA)

for providing us with breeding pairs of caPKD1 mice. We acknowledge the contribution of Emiel Beijer (Nuclear Medicine, Maastricht University) and Agnieska Strzelecka (Pharmacology, Maastricht University) for their technical support. We also appreciate the stimulating discussions with Rhonda Bassel-Duby. This work was financially supported by the transnational University Limburg (tUL), the European Community (Integrated Project LSHM-CT-2004-005272, Exgenesis) and an NWO support grant (number 91110016) 'Redefining preclinical cardiovascular imaging *in vivo*'. D.N. is the recipient of a VIDI-Innovational Research Grant from the Netherlands Organization of Scientific Research (NWO-ALW grant 864.10.007).

## References

[1] Taegtmeyer H, Passmore JM. Defective energy metabolism of the heart in diabetes. Lancet 1985;1:139–41.
[2] Nikolaidis LA, Levine TB. Peroxisome proliferator activator receptors (PPAR), insulin resistance, and cardiomyopathy: friends or foes for the diabetic patient with heart failure? Cardiol Rev 2004;12:158–70.
[3] Taegtmeyer H, McNulty P, Young ME. Adaptation and maladaptation of the heart in diabetes: part I: general concepts. Circulation 2002;105:1727–33.
[4] Carley AN, Severson DL. Fatty acid metabolism is enhanced in type 2 diabetic hearts. Biochim Biophys Acta 2005;1734:112–26.
[5] Glatz JF, Luiken JJ, Bonen A. Membrane fatty acid transporters as regulators of lipid metabolism: implications for metabolic disease. Physiol Rev 2010;90:367–417.
[6] Zorzano A, Sevilla L, Camps M, Becker C, Meyer J, Kammermeier H, et al. Regulation of glucose transport, and glucose transporters expression and trafficking in the heart: studies in cardiac myocytes. Am J Cardiol 1997;80:65A–76A.
[7] Ibrahimi A, Abumrad NA. Role of CD36 in membrane transport of long-chain fatty acids. Curr Opin Clin Nutr Metab Care 2002;5:139–45.
[8] Schwenk RW, Luiken JJ, Bonen A, Glatz JF. Regulation of sarcolemmal glucose and fatty acid transporters in cardiac disease. Cardiovasc Res 2008;79:249–58.
[9] Erion DM, Shulman GI. Diacylglycerol-mediated insulin resistance. Nat Med 2010; 16:400–2.
[10] Ilercil A, Devereux RB, Roman MJ, Paranicas M, O'grady MJ, Welty TK, et al. Relationship of impaired glucose tolerance to left ventricular structure and function: The Strong Heart Study. Am Heart J 2001;141:992–8.
[11] Dirkx E, Schwenk RW, Glatz JF, Luiken JJ, van Eys GJ. High fat diet induced diabetic cardiomyopathy. Prostaglandins Leukot Essent Fatty Acids 2011;85:219–25.
[12] Uphues I, Kolter T, Goud B, Eckel J. Failure of insulin-regulated recruitment of the glucose transporter GLUT4 in cardiac muscle of obese Zucker rats is associated with alterations of small-molecular-mass GTP-binding proteins. Biochem J 1995; 311:161–6.
[13] Viollet B, Mounier R, Leclerc J, Yazigi A, Foretz M, Andreelli F. Targeting AMP-activated protein kinase as a novel therapeutic approach for the treatment of metabolic disorders. Diabetes Metab 2007;33:395–402.
[14] Habets DD, Coumans WA, El Hasnaoui M, Zarrinpashneh E, Bertrand L, Viollet B, et al. Crucial role for LKB1 to AMPKalpha2 axis in the regulation of CD36-mediated long-chain fatty acid uptake into cardiomyocytes. Biochim Biophys Acta 2009;1791:212–9.
[15] Lint JV, Rykx A, Vantus T, Vandenheede JR. Getting to know protein kinase D. Int J Biochem Cell Biol 2002;34:577–81.
[16] Luiken JJ, Vertommen D, Coort SL, Habets DD, El Hasnaoui M, Pelsers MM, et al. Identification of protein kinase D as a novel contraction-activated kinase linked to GLUT4-mediated glucose uptake, independent of AMPK. Cell Signal 2008;20: 543–56.
[17] Dirkx E, Schwenk RW, Coumans WA, Hoebers N, Angin Y, Viollet B, et al. Protein kinase D1 is essential for contraction-induced glucose uptake but is not involved in fatty acid uptake into cardiomyocytes. J Biol Chem 2012;287:5871–81.
[18] Harrison BC, Kim MS, van Rooij E, Plato CF, Papst PJ, Vega RB, et al. Regulation of cardiac stress signaling by protein kinase d1. Mol Cell Biol 2006;26:3875–88.
[19] Huynh QK, McKinsey TA. Protein kinase D directly phosphorylates histone deacetylase 5 via a random sequential kinetic mechanism. Arch Biochem Biophys 2006;450:141–8.
[20] Olson EN, Backs J, McKinsey TA. Control of cardiac hypertrophy and heart failure by histone acetylation/deacetylation. Novartis Found Symp 2006;274:3–12.
[21] Habets DD, Coumans WA, Voshol PJ, den Boer MA, Febbraio M, Bonen A, et al. AMPK-mediated increase in myocardial long-chain fatty acid uptake critically depends on sarcolemmal CD36. Biochem Biophys Res Commun 2007;355:204–10.
[22] Luiken JJ, van Nieuwenhoven FA, America G, van der Vusse GJ, Glatz JF. Uptake and metabolism of palmitate by isolated cardiac myocytes from adult rats: involvement of sarcolemmal proteins. J Lipid Res 1997;38:745–58.
[23] Folch J, Lees M, Sloane Stanley GH. A simple method for the isolation and purification of total lipids from animal tissues. J Biol Chem 1957;226:497–509.
[24] van Bilsen M, Smeets PJ, Gilde AJ, van der Vusse GJ. Metabolic remodelling of the failing heart: the cardiac burn-out syndrome? Cardiovasc Res 2004;61:218–26.
[25] Luptak I, Yan J, Cui L, Jain M, Liao R, Tian R. Long-term effects of increased glucose entry on mouse hearts during normal aging and ischemic stress. Circulation 2007; 116:901–9.
[26] Glatz JF, Bonen A, Ouwens DM, Luiken JJ. Regulation of sarcolemmal transport of substrates in the healthy and diseased heart. Cardiovasc Drugs Ther 2006;20:471–6.
[27] Jaswal JS, Keung W, Wang W, Ussher JR, Lopaschuk GD. Targeting fatty acid and carbohydrate oxidation—a novel therapeutic intervention in the ischemic and failing heart. Biochim Biophys Acta 1813;2011:1333–50.
[28] Coort SL, Hasselbaink DM, Koonen DP, Willems J, Coumans WA, Chabowski A, et al. Enhanced sarcolemmal FAT/CD36 content and triacylglycerol storage in cardiac myocytes from obese Zucker rats. Diabetes 2004;53:1655–63.
[29] Ouwens DM, Diamant M, Fodor M, Habets DD, Pelsers MM, El Hasnaoui M, et al. Cardiac contractile dysfunction in insulin-resistant rats fed a high-fat diet is associated with elevated CD36-mediated fatty acid uptake and esterification. Diabetologia 2007;50:1938–48.
[30] Rider OJ, Nethononda R, Petersen SE, Francis JM, Byrne JP, Leeson P, et al. Concentric left ventricular remodeling and aortic stiffness: a comparison of obesity and hypertension. Int J Cardiol 2013;167:2989–94.
[31] Jaggi M, Du C, Zhang W, Balaji KC. Protein kinase D1: a protein of emerging translational interest. Front Biosci 2007;12:3757–67.
[32] LaValle CR, George KM, Sharlow ER, Lazo JS, Wipf P, Wang QJ. Protein kinase D as a potential new target for cancer therapy. Biochim Biophys Acta 1806;2010:183–92.